

## Fabrication of substrates with curvature for cell cultivation by alpha-particle irradiation and chemical etching of PADC films

C.K.M. Ng<sup>a</sup>, V.T. Tjhin<sup>a</sup>, A.C.C. Lin<sup>b</sup>, J.P. Cheng<sup>b</sup>, S.H. Cheng<sup>b</sup>, K.N. Yu<sup>a,\*</sup>

<sup>a</sup> Department of Physics and Materials Science, City University of Hong Kong, Tat Chee Avenue, Kowloon Tong, Hong Kong

<sup>b</sup> Department of Biology and Chemistry, City University of Hong Kong, Tat Chee Avenue, Kowloon Tong, Hong Kong

### ARTICLE INFO

#### Article history:

Received 16 January 2012

Available online 16 February 2012

#### Keywords:

Microfabrication  
Cell-culture substrates  
Alpha particles  
PADC  
Substrate curvature

### ABSTRACT

In the present paper, we developed a microfabrication technology to generate cell-culture substrates with identical chemistry and well-defined curvature. Micrometer-sized pits with curved surfaces were created on a two-dimensional surface of a polymer known as polyallyldiglycol carbonate (PADC). A PADC film was first irradiated by alpha particles and then chemically etched under specific conditions to generate pits with well-defined curvature at the incident positions of the alpha particles. The surface with these pits was employed as a model system for studying the effects of substrate curvature on cell behavior. As an application, the present work studied mechanosensing of substrate curvature by epithelial cells (HeLa cells) through regulation of microtubule (MT) dynamics. We used end-binding protein 3–green fluorescent protein (EB3–GFP) as a marker of MT growth to show that epithelial cells having migrated into the pits with curved surfaces had significantly smaller MT growth speeds than those having stayed on flat surfaces without the pits.

© 2012 Elsevier B.V. All rights reserved.

### 1. Introduction

Biomaterials and tissue engineering research rely on the understanding of biological processes of cells on substrates or scaffolds. Different extracellular matrix (ECM) environments provide different input signals to the cells to affect their behavior such as growth, migration and differentiation. The input signals can be classified into topographical, mechanical and chemical cues. In particular, the response of a cell to physical/mechanical attributes of the ECM is referred to as ECM mechanosensing which has emerged as an important mechanism in the studies of cell response to the ECM [1–3]. One of the topographical cues is curvature [4]. Dunn and Heath [5] found that fibroblasts responded to the substrate curvature when the latter was comparable to the cell size, and proposed that the substrate curvature could mechanically restrict the formation of certain linear bundles of microfilaments involved in cell locomotion. Dunn and Ebendal [6] proposed contact guidance on aligned collagen gels as a response to the substrate geometry. Berry et al. [7] discovered that fibroblasts apparently preferred to entering pits with larger diameters on the substrate, and suggested that the cells might be sensitive to changes in the curvature of the pit walls. Smeal et al. [8] suggested that the substrate curvature affected the direction of nerve outgrowth, while James et al. [9] suggested that it affected the lamellipodial

distribution and cell polarity. On the other hand, Rumpler et al. [10] reported that tissues grew preferentially on surfaces with higher curvatures. However, studies on the effects of curvature of substrates, in particular concave substrates, on cell behavior are still relatively scarce, which might largely due to lack of convenient methods to generate substrates with different and well-defined curvature.

The current paper proposed a microfabrication technology to generate substrates with well-defined curvature. In essence, micrometer-sized pits with curved surfaces were created on a two-dimensional (2D) surface of a polymer known as polyallyldiglycol carbonate (PADC). A PADC film was first irradiated by alpha particles and then chemically etched under specific conditions to generate pits with well-defined curvature at the incident positions of the alpha particles. The surface with these pits was employed as a model system for studying the effects of substrate curvature on cell behavior.

As an example of application, the current paper studied the microtubule dynamics of cells cultured on these substrates with curvature. MTs are polar polymers of tubulin dimers that are found in almost all eukaryotic cells. They are cytoskeletal filaments which have a fundamental role in cell division, intracellular trafficking, cell motility, as well as in development and maintenance of cell shape [11]. In many cell types, MTs are organized in a radial array with their minus-ends anchored at the centrosome and their plus-ends extending toward the cell periphery where they are involved in a number of essential cellular events [12–14]. MTs are

\* Corresponding author. Tel.: +852 34427812; fax: +852 34420538.

E-mail address: [peter.yu@cityu.edu.hk](mailto:peter.yu@cityu.edu.hk) (K.N. Yu).

highly dynamic and undergo phases of growth and shrinkage stochastically (dynamic instability), and move continuously through the cytoplasm. This facilitates contacts between MT ends and relatively stationary structures such as chromosomes and focal adhesions, and allows the cell to react to external cues [15,16]. In neurons, MTs and their dynamic instability are required for neurite initiation and extension, elaboration of the growth cone, and axonal branching [17,18]. More recently, Myers et al. [19] showed that specific parameters of MT assembly dynamics, growth speed and growth persistence, were globally and regionally modified by and contributed to ECM mechanosensing. Indeed, there were evidences that MTs were regulated by ECM mechanosensing and might also mediate morphological responses to mechanosensing [20,21].

Live imaging studies have shown that an increasing number of MT regulatory proteins from various organisms specifically associates with the distal ends of growing MTs. Many researches were performed on the behavior of plus end-binding proteins (also called “plus end-tracking proteins” or +TIPs), fused to GFP (green fluorescent protein) (GFP + TIPs), in non-neuronal cells. Stepanov et al. [22] used end-binding protein 3–green fluorescent protein (EB3–GFP) as a marker of growing plus-end of MTs to visualize the MT growing ends. MT growth speeds were determined by tracking EB3–GFP comets at MT plus-ends [22]. In the present work, we studied the MT dynamics of live epithelial cells (HeLa cells) on substrates with curvature (in comparison to those on flat substrates) using EB3–GFP as a marker of growing distal tips of MTs. HeLa cells were transfected with the plasmid expressing EB3–GFP. The MT growth speeds in the HeLa cells were determined from time-lapse live images obtained using confocal laser scanning microscope.

## 2. Materials and methods

### 2.1. Microfabrication of substrates with curvature

In the present work, PADC films with a thickness of 1 mm from Page Moldings (Pershore) Limited, Worcestershire, were employed to fabricate the substrates with or without curvature for cell cultivation. PADC films with a size of  $2 \times 2 \text{ cm}^2$  were prepared, irradiated with 5 MeV alpha particles from an  $^{241}\text{Am}$  alpha-particle source and then subsequently chemically etched in a 6.25 N aqueous NaOH solution at 70 °C for 30 h (which was the most commonly employed conditions, giving a bulk etch rate of  $\sim 1.2 \mu\text{m/h}$  [23]). On the other hand, control flat substrates were also prepared which were unirradiated films but underwent the same etching procedures. After chemical etching in NaOH solutions, both irradiated and unirradiated etched PADC films were further etched for 5 min in 1 N NaOH/ethanol at 40 °C (with a bulk etch rate of  $\sim 9.5 \mu\text{m/h}$  [24]). This final step of etching in NaOH/ethanol led to better biocompatibility of the films [25]. Upon chemical etching, pits were formed in the irradiated films. The pits were already in the spherical phase so that the latent tracks of damages in the polymer inflicted by the alpha particles had been etched away, and thus the flat and the curved parts of the substrate surface would have the same chemical composition [26–28]. The dimensions of these etched pits were measured experimentally using a surface profilometer (Form Talysurf PGI Profilometer, Taylor Hobson, England).

### 2.2. Cell culture

HeLa cervix cancer cells were obtained from the American Type Culture Collection. HeLa cells were cultured on the  $2 \times 2 \text{ cm}^2$  PADC substrates with different treatments as described in Section 2.1.

Before cell culture, the substrates were sterilized by submerging in 75% (v/v) ethyl alcohol for 2 h and then washed by PBS. These films were then used for HeLa cell culture. The HeLa cells were maintained as exponentially growing monolayer at low-passage numbers in Dulbecco's modified eagle medium (D-MEM) supplemented with 10% fetal bovine serum. The cells were cultured at 37 °C in humidified atmosphere containing 5%  $\text{CO}_2$ . Sub-cultivation was performed every 3–4 days. The cells were trypsinized with 0.5/0.2% (v/v) trypsin/EDTA (ethylenediamine-tetra-acetic acid; Gibco), adjusted to  $4 \times 10^5$  cells in 3 ml medium and plated out on the substrates placed inside a 35 mm diameter Petri dish. All cells were allowed to plate out on the substrates for 1 day.

### 2.3. EB3–GFP transfection, imaging and video analysis

One day after cell seeding, the cells on the substrates were transfected with the plasmid expressing EB3–GFP (supplied by Dr. Roger Y. Tsien of University of California, San Diego) using Lipofectamine 2000 (Invitrogen). After 1 day post-transfection, time-lapse images were captured using a confocal laser scanning microscope (Leica TCS SP5) with 100 $\times$  objectives in a 37 °C chamber for live cells on the substrates. The images were acquired every 4 s. Quantitative analysis of the MT dynamics was carried out on the time-lapse movies of cells expressing EB3–GFP. The MT growth speeds were obtained by tracking the EB3–GFP comets at the MT plus ends using the MetaMorph version 7.0 software (Molecular Devices Corporation, US).

## 3. Results

### 3.1. Characterization of etched pits

The three-dimensional profile obtained using a surface profilometer for an etched pit is shown in Fig. 1(a–c). The opening diameter and depth were  $50.7 \pm 0.4$  and  $18.8 \pm 0.2 \mu\text{m}$ , respectively. The volume and the surface area of the pit were determined as  $22400 \pm 300 \mu\text{m}^3$  and  $3000 \pm 60 \mu\text{m}^2$ . The average volume and surface-to-volume ratio of a HeLa cell were estimated as  $2600 \mu\text{m}^3$  [29] and  $0.48 \pm 0.1 \mu\text{m}^{-1}$  [30], respectively. Therefore, the surface area of a HeLa cell could be calculated as  $1250 \pm 260 \mu\text{m}^2$ . As such, the surface area and the volume of a single pit were about 2.4 times and 8.6 times those of the average cell area and volume, respectively. In other words, the pit could easily accommodate an entire cell. The size of the pits was important for our design of the curved substrates. If the pits were too large, the curvature might be too small and the substrates would resemble a flat one. It is recalled that fibroblasts responded to the substrate curvature when the latter was comparable to the cell size [5]. On the contrary, if the pits were too small, they could not hold an entire cell and the cell might mechanosense a major part of a flat substrate.

### 3.2. Visualization of growing microtubule

Fig. 2 shows representative images of live HeLa cells plated out on the flat parts and in pits on the PADC substrates for 2 days (1 day post transfection of EB3–GFP). The green-dash/comet-like signals of growing MT plus-ends generally moved radially from the cell center to the periphery of cells in the fluorescent images captured at 4 s per frame as illustrated in Fig. 2(a). Fig. 2(b) shows the corresponding images of cells captured in the optical transmission mode.

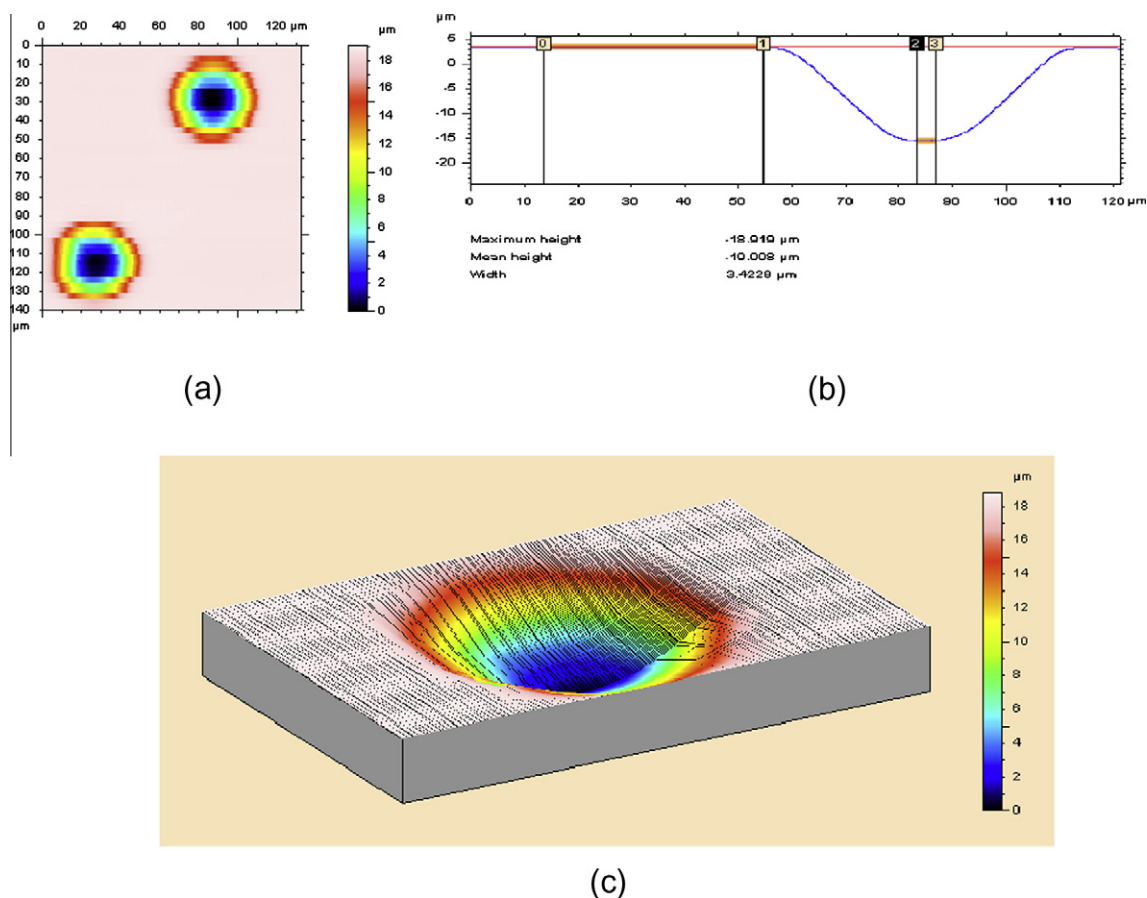


**Fig. 1.** The profile of an etched pit in a PADC film generated by a normally incident 5 MeV alpha particle and subsequent chemical etching (in a 6.25 N aqueous NaOH solution at 70 °C for 30 h and then in 1 N NaOH/ethanol at 40 °C for 5 min) recorded using a surface profilometer. (a) Top view; (b) cross-sectional view; (c) 3D view. Adopted from Ref. [42].

### 3.3. Analysis of EB3–GFP movements

In the present analysis, all fluorescent movements were included irrespective of the number of consecutive frames in which they appeared. Fig. 3 shows an example of measurements of growing MT movements in the cells. The EB3–GFP movements were analyzed by time-lapse microscopy. We analyzed a total number of 29 cells (15 cells on flat surfaces; 14 cells in pits) with a total of 960 EB3–GFP dashes traced (388 and 572 tracks corresponding to pits and flat surfaces, respectively). The images were acquired about every 4 s. EB3–GFP dashes in the HeLa cells which could be followed in more than three consecutive frames were studied. Fig. 4 illustrated the movement of EB3–GFP comet on MT tip growing. EB3 tracks (red) were obtained by EB3–GFP patch distance during 12 s. The speeds of EB3–GFP comets were determined by the ratios of total distance/total time.

For each set of experiment, one flat substrate and one substrate with pits were used. A total of three sets of experiments were carried out, so six substrates were involved. Here, (1) the mean MT growth speed for each cell was first calculated; (2) for each set of experiment, the mean MT growth speed from individual cells was then computed, and (3) finally the mean and SD for the means from different sets of experiment were determined. The average MT growth speeds in cells plated out in pits and on flat surfaces were determined as  $13 \pm 3$  and  $16 \pm 4$   $\mu\text{m}/\text{min}$ , respectively. Fig. 5 illustrated the fold change of average speeds, with the values for pits and flat surfaces as  $1.00 \pm 0.12$  and  $1.25 \pm 0.18$ , respectively. The results show a significant decrease of  $25 \pm 5\%$  in the average MT growth speed when the cells were plated out in pits,

when compared with flat surfaces ( $p < 0.001$ ,  $n = 3$ , obtained using  $t$ -test).

## 4. Discussion

A special microfabrication technology was proposed in the present work to generate substrates with well-defined curvature. PADC films were first irradiated by alpha particles and then chemically etched under specific conditions to create micrometer-sized pits with curved surfaces on these films. The pit diameters allowed the cells to completely enter the pits so these cells did not mechanosense a major part of the flat substrate surface, which allowed us to focus on the effects of curvature alone.

ECM mechanosensing has become an important mechanism in the studies of cell response to the ECM. For example, ECM mechanosensing was suggested as a regulator of endothelial cell branching morphogenesis and motility [1,2,19,31]. Although substrate curvature has been recognized as a topographical cue, convenient methods to generate substrates with different and well-defined curvature have been lacking, which might have led to the relatively few investigations on the effects of curvature of substrates on the cell behavior.

MTs are part of the structural scaffold of the cell and serve as tracks along which organelles, vesicles, and large molecules are transported [15,32]. MTs and their dynamic instability are essential for various cellular processes, including development, division, cell shape formation, cell polarization and motility [15,29,30,33–39]. Our results revealed the mechanosensing of substrate curvature



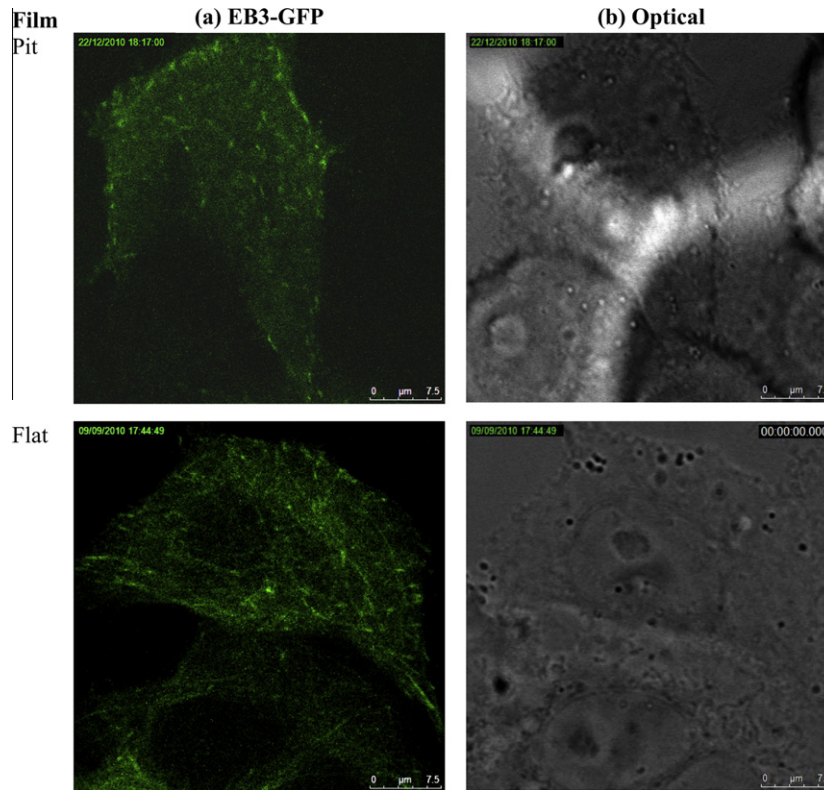


**Fig. 2.** Visualization of growing microtubule plus-ends in expressing EB3-GFP of cells in a pit and on a flat surface using time-lapse mode of confocal microscope. Bar = 7.5  $\mu\text{m}$ .

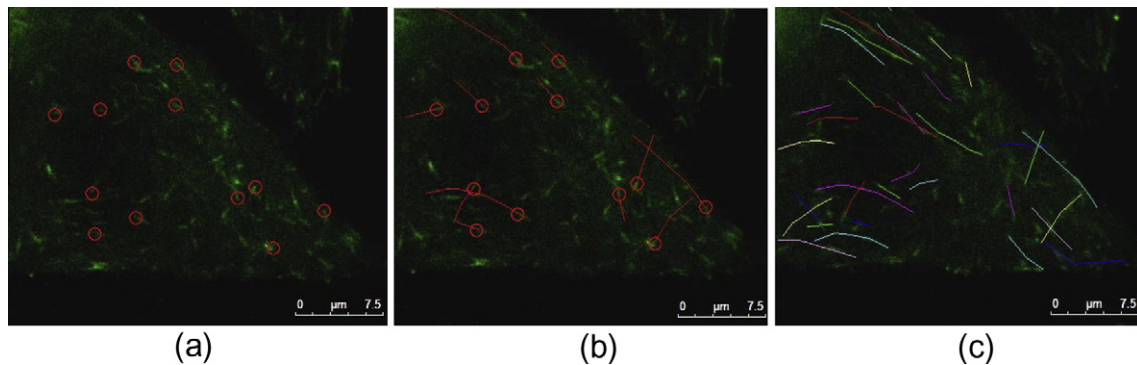


**Fig. 3.** Microtubule movement determination. (a) EB3-GFP patches were marked with red circles for analyses; (b) EB3 tracks obtained by EB3-GFP patches displacement on time-lapse series (maximum number of consecutive frames were assessed for individual patches); (c) all tracks (in different colors) can be determined in the whole series (generally a total of time span of 1–2 min for each complete series). Bar = 7.5  $\mu\text{m}$ . (For interpretation of the references to color in this figure legend, the reader is referred to the web version of this article.)

by epithelial cells. Studies of time-lapse live imaging of EB3-GFP using confocal laser scanning microscope showed that the epithelial cells having migrated into the pits with curved surfaces had significantly smaller MT growth speeds than those having stayed on flat surfaces without the pits. The present results showed that MT dynamics in epithelial cells were regulated when the cells engaged a curved ECM in pits.

Berry et al. [7] studied the fibroblast motility on 2D quartz substrates with regular pits (vertical walls with heights of 4.8  $\mu\text{m}$ ; flat circular bases with diameters of 7, 15 and 25  $\mu\text{m}$ ; and separated at 20 and 40  $\mu\text{m}$ ) and observed an intriguing preference for the cells to enter the pits with larger diameters. Since the cells could not know the pit dimensions before entering it, this preference was likely related to the mechanosensing of substrate curvature (of

the vertical pit walls). Another previous study also showed that lymphocytes could migrate into serum-coated micropore filters with pore sizes of 3 or 8  $\mu\text{m}$ , but could not migrate into filters with smaller pores (0.22 or 0.45  $\mu\text{m}$ ) [40].

For tissue engineering purposes, 3D porous scaffolds are often deployed as templates for initial cell attachment and subsequent tissue formation [41]. Incidentally, the substrates with pits with defined curvature fabricated in the present work resembled in some ways the structure of these 3D scaffolds in that the latter also consisted of pores with defined curvature as their basic structural element. As such, substrates with pits with different curvature could be created and employed to provide guiding information on 3D scaffolds. The cell types involved in the tissue engineering could be cultured on these substrates and studied for, e.g., cell

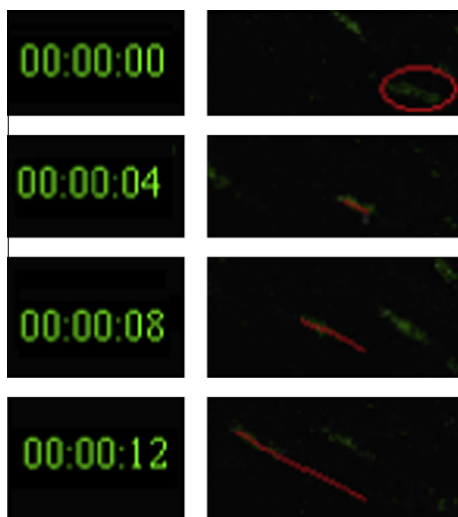


**Fig. 4.** High magnification of four consecutive frames (0–12 s) showing the movement of an EB3–GFP comet on the tip of a growing microtubule. EB3 tracks (red) were obtained from the EB3–GFP patches. (For interpretation of the references to color in this figure legend, the reader is referred to the web version of this article.)

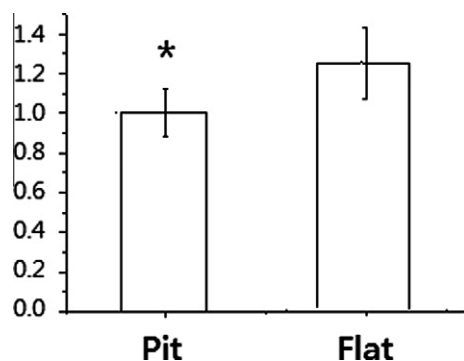


**Fig. 5.** Normalized microtubule growth speeds in cells cultured in pits and on flat surfaces. Error bars represent one SDs (\* $p < 0.001$ ,  $n = 3$ ).

migration and penetration. The desirable scaffold could then be chosen and fabricated according to these results to minimize the risk of scaffold failure.

## 5. Conclusions

- (1) We developed a microfabrication technology to generate cell-culture substrates with identical chemistry and well-defined curvature.
- (2) We used EB3–GFP as a marker of MT growth to show that the MT growth speed in epithelial cells was modified by the curvature of the underlying substrate. MT growth speeds were determined by tracking EB3–GFP comets at MT plus-ends.

- (3) We observed that the epithelial cells having engaged a substrate with curvature had significantly smaller MT growth speeds.

## References

- [1] D.E. Ingber, *Circ. Res.* 91 (2002) 877–887.
- [2] K. Ghosh, C.K. Thodeti, A.C. Dudley, A. Mammoto, M. Klagsbrun, D.E. Ingber, *Proc. Nat. Acad. Sci.* 105 (2008) 11305–11310.
- [3] A. Mammoto, K.M. Connor, T. Mammoto, C.W. Yung, D. Huh, C.M. Aderman, G. Mostoslavsky, L.E.H. Smith, D.E. Ingber, *Nature* 457 (2009) 1103–U57.
- [4] U.S. Schwarz, I.B. Bischofs, *Med. Eng. Phys.* 27 (2005) 763–772.
- [5] G.A. Dunn, J.P. Heath, *Exp. Cell Res.* 101 (1976) 1–14.
- [6] G.A. Dunn, T. Ebdal, *Exp. Cell Res.* 111 (1978) 475–479.
- [7] C.C. Berry, G. Campbell, A. Spadicino, M. Robertson, A.S.G. Curtis, *Biomaterials* 25 (2004) 5781–5788.
- [8] R.M. Smeal, R. Rabbitt, R. Biran, P.A. Tresco, *Ann. Biomed. Eng.* 33 (2005) 376–382.
- [9] J. James, E.D. Goluch, H. Hu, C. Liu, M. Mrksich, *Cell Mot. Cytos.* 65 (2008) 841–852.
- [10] M. Rumpler, A. Woesz, J.W.C. Dunlop, J.T. van Dongen, P. Fratzl, *J.R. Soc. Interface* 5 (2008) 1173–1180.
- [11] D. Bray, in: M. Day (Ed.), *Cell Movement: From Molecules to Motility*, second ed., Garland Publishing, New York, 2001, 400 pp.
- [12] M. Moritz, D.A. Agard, *Curr. Opin. Struct. Biol.* 11 (2001) 174–181.
- [13] J. Howard, A.A. Hyman, *Nature* 422 (2003) 753–758.
- [14] A. Akhmanova, C.C. Hoogenraad, *Curr. Opin. Cell Biol.* 17 (2005) 47–54.
- [15] A. Desai, T.J. Mitchison, *Ann. Rev. Cell Dev. Biol.* 13 (1997) 83–117.
- [16] T. Mitchison, M. Kirschner, *Nature* 312 (1984) 237–242.
- [17] E.W. Dent, K. Kalil, *J. Neurosci.* 21 (2001) 9757–9769.
- [18] L. Dehmelt, F.M. Smart, R.S. Ozer, S. Halpain, *J. Neurosci.* 23 (2003) 9479–9490.
- [19] K.A. Myers, K.T. Applegate, G. Danuser, R.S. Fischer, C.M. Waterman, *J. Cell Biol.* 192 (2011) 321–334.
- [20] I. Kaverina, O. Krylyshkina, K. Beningo, K. Anderson, Y.L. Wang, J.V. Small, *J. Cell Sci.* 115 (2002) 2283–2291.
- [21] S. Rhee, H. Jiang, C.H. Ho, F. Grinnell, *Proc. Nat. Acad. Sci.* 104 (2007) 5425–5430.
- [22] T. Stepanova, J. Slemmer, C.C. Hoogenraad, G. Lansbergen, B. Dortland, C.I. De Zeeuw, F. Grosveld, G. van Cappellen, A. Akhmanova, N. Galjart, *J. Neurosci.* 23 (2003) 2655–2664.
- [23] J.P.Y. Ho, C.W.Y. Yip, D. Nikezic, K.N. Yu, *Radiat. Meas.* 36 (2003) 141–143.
- [24] K.F. Chan, F.M.F. Ng, D. Nikezic, K.N. Yu, *Nucl. Instr. Meth. B* 263 (2007) 284–289.
- [25] W.Y. Li, K.F. Chan, A.K.W. Tse, W.F. Fong, K.N. Yu, *Nucl. Instr. Meth. B* 248 (2006) 319–323.
- [26] D. Nikezic, K.N. Yu, *Mater. Sci. Eng., R* 46 (2004) 51–123.
- [27] D. Nikezic, K.N. Yu, *Radiat. Meas.* 37 (2003) 39–45.
- [28] D. Nikezic, K.N. Yu, *Comput. Phys. Commun.* 174 (2006) 160–165.
- [29] O.C. Rodriguez, A.W. Schaefer, C.A. Mandato, P. Forscher, W.M. Bement, C.M. Waterman-Storer, *Nat. Cell Biol.* 5 (2003) 599–609.
- [30] J.V. Small, B. Geiger, I. Kaverina, A. Bershadsky, *Nat. Rev. Mol. Cell Biol.* 3 (2002) 957–964.
- [31] R.S. Fischer, M. Gardel, X. Ma, R.S. Adelstein, C.M. Waterman, *Curr. Biol.* 19 (2009) 260–265.
- [32] M. Schliwa, G. Woehlke, *Nature* 422 (2003) 759–765.
- [33] J.V. Small, I. Kaverina, *Curr. Opin. Cell Biol.* 15 (2003) 40–47.
- [34] A.D. Bershadsky, N.Q. Balaban, B. Geiger, *Annu. Rev. Cell Dev. Biol.* 19 (2003) 677–695.
- [35] A.D. Bershadsky, C. Ballestrem, L. Carramusa, Y. Zilberman, B. Gilquin, S. Khochbin, A.Y. Alexandrova, A.B. Verkhovskiy, T. Shemesh, M.M. Kozlov, *Eur. J. Cell Biol.* 85 (2006) 165–173.
- [36] J.M. Schober, Y.A. Komarova, O.Y. Chaga, A. Akhmanova, G.G. Borisov, *J. Cell Sci.* 120 (2007) 1235–1244.
- [37] M. Prager-Khoutorsky, I. Goncharov, A. Rabinkov, D. Mirelman, B. Geiger, A.D. Bershadsky, *Cell Motil. Cytoskeleton* 64 (2007) 321–337.
- [38] A. Efimov, A. Kharitonov, N. Efimova, J. Loncarek, P.M. Miller, N. Andreyeva, P. Gleeson, N. Galjart, A.R.R. Maia, I.X. McLeod, J.R. Yates, H. Maiato, A. Khodjakov, A. Akhmanova, I. Kaverina, *Dev. Cell* 12 (2007) 917–930.
- [39] J.A. Broussard, D.J. Webb, I. Kaverina, *Curr. Opin. Cell Biol.* 20 (2008) 85–90.
- [40] W.S. Haston, J.M. Shields, P.C. Wilkinson, *J. Cell Biol.* 92 (1982) 747–752.
- [41] D.W. Huttmacher, *J. Biomater. Sci. Polym. Ed.* 12 (2001) 107–124.
- [42] C.K.M. Ng, J.P. Cheng, S.H. Cheng, K.N. Yu, *Nucl. Instr. Meth. A* 619 (2010) 401–407.